# Quantum synchronization and quantum $\varphi$ synchronization in a coupled optomechanical system with Kerr nonlinearity

J. T. Sun, H. D. Liu,* and X. X. Yi

*Center for Quantum Sciences and School of Physics, Northeast Normal University, Changchun 130024, China*

(Received 16 September 2023; revised 28 December 2023; accepted 11 January 2024; published 1 February 2024)

In this work, we study the quantum synchronization and quantum $\phi$ synchronization of two mechanical oscillators in a coupled optomechanical system. The oscillators are coupled to an optical cavity filled with a Kerr nonlinear medium and subjected to periodic modulation of the cavity detunings and driving amplitudes by a common driving field. Our results show that the quantum synchronization and quantum $\phi$ synchronization in nonlinear systems exhibit more favorable behaviors than in linear systems. In addition, we have investigated the performances of two synchronization measurements to various parameters by analyzing the sensitivity of $\phi$. Accordingly, perfect synchronization can be achieved under specific parameters by periodically modulating the cavity and driving field. Our findings could offer insights into other quantum effects and pave the way for studying quantum correlations.

DOI: 10.1103/PhysRevA.109.023502

## I. INTRODUCTION

Classical synchronization is an intriguing and universal phenomenon that dates back to the 17th century when Huygens observed the synchronization phenomenon of two pendulum clocks with a common support [1]. Since then, synchronization has been widely observed and studied in classical systems. These complex systems share a common feature in that synchronization can be achieved through mutual interaction rather than exterior driving field [2]. However, extending synchronization concepts from the classical to the quantum regime is not a direct analogy since quantum coordinates and momenta are constrained by the Heisenberg uncertainty principle. Mari *et al.* proposed the concept of quantum synchronization and quantum phase synchronization and developed a quantum synchronization measurement [2] to generalize the concept of classical synchronization into continuous-variable quantum systems. Optomechanical systems are often studied to explore quantum synchronization due to their necessary properties for spontaneous synchronization, such as existing nonlinear dynamics of optomechanical coupling and limit cycles [3,4]. Subsequently, quantum synchronization has been widely used in cavity quantum electrodynamics [5,6], atomic ensembles [7–9], van der Pol (vdP) oscillators [6,10–12], Bose-Einstein condensation [13], superconducting circuit systems [14,15], and so on. In addition, quantum synchronization can also be used to achieve communication in complex networks [16–18]. Sensor [19,20] and encryption [21–23] communication are common applications that use quantum synchronization.

Moreover, some studies have investigated whether quantum synchronization has some correlations with other properties, for example, mutual information [6], quantum discord [24], and entanglement [25–27]. The essence of these characteristics is the interaction of subsystems. And quantum correlations are regarded as a signal to represent quantum synchronization [28–30]. In addition, there are several ways to enhance quantum synchronization and other correlations. Periodic modulation can be used as a common method and exerting modulation on a cavity is better than a driving field [31–33]. In addition, the quadratic optomechanical coupling is confirmed to enhance phase synchronization between two mechanical oscillators with different frequencies in a nonlinear system [34]. Later, some studies opened up a new direction for using exceptional points to investigate the collective phenomenon in a nonlinear system, such as chaos [35]. And other interesting collective phenomena related to quantum synchronization, such as phase synchronization [36–39] and frequency locking [40,41], have also received attention in the past decades. Recently, Bohmian trajectories have been used to study how the quantum synchronization of discrete variables can signal the level of synchronization more intuitively [42].

Based on the measure of quantum synchronization proposed by Mari *et al.*, subsequently, quantum $\phi$ synchronization as a more generalized measure is proposed when mean values are out of synchronization, and quantum synchronization is regarded as a special case of quantum $\phi$ synchronization when $\phi = 0$ [43]. Thus, it is worth studying the distinction and correlation between quantum synchronization and quantum $\phi$ synchronization in nonlinear optomechanical systems. We want to know how to achieve synchronization of mean values and enhance quantum $\phi$ synchronization and quantum synchronization. In addition, the response of two synchronization measures to different parameters is unknown, and whether the phase difference $\phi$ between the two mechanical oscillators is susceptible to different parameters. To clarify these questions, we propose a scheme for the response of two synchronization measures in a coupled

*liuhd100@nenu.edu.cn

 

optomechanical system, where two mechanical oscillators are optomechanically coupled to a cavity and two oscillators are coupled through phonon tunneling to each other. After some numerical simulation and detailed analysis, we have found that the behaviors of quantum $\phi$ synchronization and quantum synchronization are quite different due to the existence of a phase difference $\phi$ between the two mechanical oscillators. Moreover, quantum $\phi$ synchronization is sensitive to some specific parameters; accordingly, we have found the optimal parameters to achieve perfect quantum synchronization and quantum $\phi$ synchronization.

The general structure of the paper is as follows. In Sec. II, we first introduce the definition of quantum synchronization and quantum $\phi$ synchronization. In Sec. III A, we propose a theoretical model that consists of a cavity and two mechanical oscillators with different frequencies, and then we calculate the dynamics of the system. In Sec. III B, synchronization of mean values can be achieved by directly coupling two oscillators and quantum $\phi$ synchronization can be enhanced, so perfect synchronization is shown under certain parameters. In Sec. III C, we study the response of quantum synchronization and quantum $\phi$ synchronization corresponding to different parameters. In Sec. III D, we give a brief discussion of the experimental realization of the investigated optomechanical system. In Sec. IV, we give a summary and conclusion.

## II. QUANTUM SYNCHRONIZATION AND QUANTUM $\phi$ SYNCHRONIZATION MEASURES

Unlike the straightforward task of measuring synchronization in a classical system, extending synchronization concepts from the classical to the quantum regime is not a direct analogy since quantum coordinates and momenta (dimensionless quantities) are constrained by the canonical commutation rules $[q_j(t), p_{j'}(t)] = i\delta_{jj'}$. The insights of Mari *et al.* were that we can use this restriction to define the measurement of quantum synchronization as [2]

$$S_c = \frac{1}{\langle q_-(t)^2 + p_-(t)^2\rangle}, \tag{1}$$

where $q_-(t) = \frac{1}{\sqrt{2}}[q_1(t) - q_2(t)]$ and $p_-(t) = \frac{1}{\sqrt{2}}[p_1(t) - p_2(t)]$ are synchronization errors, and the evolution of $S_c$ is described by the dimensionless canonical variables $q_j(t)$ and $p_j(t)$ [2]. According to the Heisenberg principle, $S_c$ goes from classical to the quantum regime by excluding the mean values of the operators $(\langle q_-(t)\rangle, \langle p_-(t)\rangle)$ by redefining the variables as

$$\begin{aligned} q_-(t) &\to \delta q_-(t) = q_-(t) - \langle q_-(t)\rangle, \\ p_-(t) &\to \delta p_-(t) = p_-(t) - \langle p_-(t)\rangle. \end{aligned} \tag{2}$$

When

$$\langle q_-(t)\rangle = \langle p_-(t)\rangle = 0, \tag{3}$$

i.e., the mean value is synchronized [16], the above measurement of quantum synchronization becomes

$$S_q = \frac{1}{\langle \delta q_-(t)^2 + \delta p_-(t)^2\rangle}, \tag{4}$$

with $S_q \in (0, 1]$, and the perfect quantum synchronization is achieved when $S_q = 1$. However, this measure cannot intuitively study quantum antisynchronization or synchronization with arbitrary phase differences, which also have their application scenarios and practical possibilities. One feasible solution to this problem is to generalize the definition of quantum synchronization into the quantum $\phi$ synchronization [43] by redefining the error operators as

$$\begin{aligned} q_-^{\phi}(t) &= \frac{1}{\sqrt{2}}\big[q_1^{\phi}(t) - q_2^{\phi}(t)\big], \\ p_-^{\phi}(t) &= \frac{1}{\sqrt{2}}\big[p_1^{\phi}(t) - p_2^{\phi}(t)\big], \end{aligned} \tag{5}$$

with

$$\begin{aligned} q_j^{\phi}(t) &= q_j(t)\cos(\phi_j) + p_j(t)\sin(\phi_j), \\ p_j^{\phi}(t) &= p_j(t)\cos(\phi_j) - q_j(t)\sin(\phi_j). \end{aligned} \tag{6}$$

The phase $\phi_j = \arctan[\langle p_j(t)\rangle/\langle q_j(t)\rangle]$ ($\phi_j \in [0, 2\pi]$). Consequently, the measure of quantum $\phi$ synchronization takes the form [43]

$$S_\phi = \frac{1}{\langle q_-^{\phi}(t)^2 + p_-^{\phi}(t)^2\rangle}. \tag{7}$$

The limit of $S_\phi$ is also (0,1), as dictated by the Heisenberg principle. By taking the changes in variables,

$$\begin{aligned} q_-^{\phi}(t) &\to \delta q_-^{\phi}(t) = q_-^{\phi}(t) - \langle q_-^{\phi}(t)\rangle, \\ p_-^{\phi}(t) &\to \delta p_-^{\phi}(t) = p_-^{\phi}(t) - \langle p_-^{\phi}(t)\rangle, \end{aligned} \tag{8}$$

when the average amplitude and period of the mean value of the two variables are the same, the above quantum $\phi$ synchronization becomes

$$S_q^{\phi} = \frac{1}{\big\langle \delta q_-^{\phi}(t)^2 + \delta p_-^{\phi}(t)^2\big\rangle}, \tag{9}$$

where $\phi = \phi_2 - \phi_1$ denotes the phase difference of two oscillators which can be determined in the following two different ways: (a) A fixed $\phi$ configuration, in which the quantum $\phi$ synchronization can be used to study a fixed $\phi$ phase difference, and the quantum (anti)synchronization can be regarded as the special case of the quantum $\phi$ synchronization for $\phi = 0$ ($\pi$); (b) $\phi = \arctan[\langle p_2\rangle/\langle q_2\rangle] - \arctan[\langle p_1\rangle/\langle q_1\rangle]$ is derived by the mean value of coordinates and momenta on the steady state. In this case, we no longer need the necessary condition of mean-value synchronization to study $\phi$ and we can also measure the changes in phase difference with different parameters.

## III. THE QUANTUM $\phi$ SYNCHRONIZATION IN A COUPLED OPTOMECHANICAL SYSTEM WITH KERR NONLINEARITY

### A. The dynamics of the optomechanical system with Kerr nonlinearity

To demonstrate the phase characteristics of quantum $\phi$ synchronization and its distinctions from classical quantum synchronization, we consider a coupled optomechanical system containing a Kerr-type nonlinear medium [31,33]. The system consists of two mechanical oscillators and a single cavity driven by a time-periodical modulated laser with

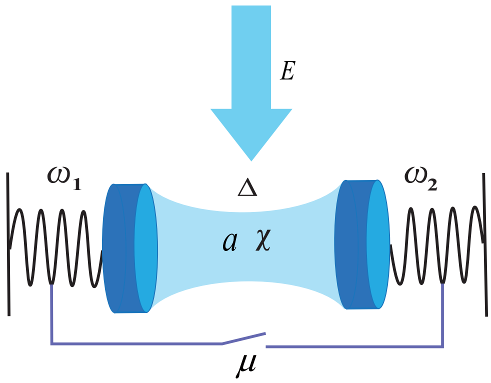


FIG. 1. Schematic illustration of the optomechanical system with two mechanical oscillators of different frequencies coupled to the same optical cavity filled with Kerr nonlinear medium. The whole system is excited by the driving field with periodical modulation. The two mechanical oscillators are coupled through phonon tunneling described by the parameter $\mu$.

frequency $\omega_L$ and intensity $E$, as shown in Fig. 1. The whole system can achieve self-sustained limit-cycle oscillation [4,44–46]. Its Hamiltonian can be written as ($\hbar = 1$) [47]

$$\begin{aligned} H =& -\Delta[1+\eta_c\cos(\Omega_c t)]a^\dagger a \\ &+ \sum_{j=1}^{2}\left\{\frac{\omega_j}{2}(p_j^2+q_j^2) - g a^\dagger a q_j\right\} \\ &+ iE[1+\eta_D\cos(\Omega_D t)](a^\dagger - a) - \chi(a^\dagger a)^2 - \mu q_1 q_2, \end{aligned} \tag{10}$$

where $a^\dagger$ and $a$ are the dimensionless creation and annihilation operators of the cavity with frequency $\omega_c$, and $q_j$ ($p_j$) represents the dimensionless position (momentum) operator of the $j$th mechanical oscillator with frequency $\omega_j$, respectively [48,49]. $\Delta$ denotes the detuning of the laser from the cavity, which is modulated with a common frequency $\Omega_c$ and amplitude $\eta_c$. $g$ is the optomechanical coupling constant. The driving laser has a time modulation of frequency $\Omega_D$ and amplitude $\eta_D$. $\chi$ is the Kerr nonlinear coefficient, and the interaction of the two mechanical oscillators is described by coupling intensity $\mu$ [2,50,51]. We shall take $\omega_1 = 1$ as a reference unit and, from now on, all the parameters are evaluated in units of $\omega_1$.

To study the time evolution of relevant variables, we use the Heisenberg-Langevin equation and consider the dissipation effects in the system [4,33,52,53]. The dynamic of operators $q_j, p_j, a$ of the system can be derived as

$$\begin{aligned} \dot{q}_j &= \omega_j p_j, \\ \dot{p}_j &= -\omega_j q_j - \gamma_j p_j + g a^\dagger a + \mu q_{3-j} + \xi_j, \\ \dot{a} &= -\{\kappa - i\Delta[1+\eta_c\cos(\Omega_c t)]\}a + igaq_j \\ &\quad + E[1+\eta_D\cos(\Omega_D t)] + i\chi(a^\dagger a + a a^\dagger)a + \sqrt{2\kappa}a^{\text{in}}, \end{aligned} \tag{11}$$

where $\kappa$ is the decay rate of the cavity [54,55] and $\gamma_j$ is the mechanical damping rate. $a^{\text{in}}$ denotes the vacuum optical noise satisfying the correlation function $\langle a^{in\dagger}(t)a^{\text{in}}(t') + a^{\text{in}}(t')a^{in\dagger}(t)\rangle = \delta(t-t')$. $\xi_j$ denotes the Brownian noise operator which satisfies the correlation function $\frac{1}{2}\langle \xi_j(t)\xi_{j'}(t') + \xi_{j'}(t')\xi_j(t)\rangle = \gamma(2\bar{n}_{\text{bath}}+1)\delta_{jj'}\delta(t-t')$ in the case of large mechanical quality $Q_m^j = \omega_j/\gamma_j \gg 1$ [56–58]. $\bar{n}_{\text{bath}} = 1/[\exp(\hbar\omega_j/k_B T) - 1]$ is the mean occupation number of the mechanical baths [56–58]. To study the mean and fluctuation dynamics of the system, we use the mean-field treatment [52,59–62] to divide each operator into a mean value and a small fluctuation and derive the linear equations (fluctuation parts) and nonlinear equations (mean value parts) [52,59–61]. By decomposing the operators in the Hamiltonian $H$ into mean values and small fluctuations, i.e.,

$$a(t) = \alpha(t) + \delta a(t), \quad O_j(t) = \bar{O}_j(t) + \delta O_j \quad (O = q, p), \tag{12}$$

and substitute them into Eq. (11), we obtain the mean value equations,

$$\begin{aligned} \dot{\bar{q}}_j &= \omega_j \bar{p}_j, \\ \dot{\bar{p}}_j &= -\omega_j \bar{q}_j - \gamma_j \bar{p}_j + g|\alpha|^2 + \mu \bar{q}_{3-j}, \\ \dot{\alpha} &= -\{\kappa - i\Delta[1+\eta_c\cos(\Omega_c t)]\}\alpha + ig\alpha\bar{q}_j \\ &\quad + E[1+\eta_D\cos(\Omega_D t)] + 2i\chi|\alpha|^2\alpha, \end{aligned} \tag{13}$$

and the equations for quantum fluctuations,

$$\begin{aligned} \delta\dot{q}_j &= \omega_j \delta p_j, \\ \delta\dot{p}_j &= -\omega_j\delta q_j - \gamma_j \delta p_j + g(\alpha\delta a^\dagger + \alpha^*\delta a) + \mu\delta q_{3-j} + \xi_j, \\ \delta\dot{a} &= -\{\kappa - i\Delta[1+\eta_c\cos(\Omega_c t)]\}\delta a + ig(\alpha\delta q_j + \bar{q}_j\delta a) \\ &\quad + 2i\chi(2|\alpha|^2\delta a + \alpha^2\delta a^\dagger) + \sqrt{2\kappa}a^{\text{in}}. \end{aligned} \tag{14}$$

In Eq. (14), we have ignored the second-order smaller terms of the fluctuation equations. By defining $u = (\delta x, \delta y, \delta q_1, \delta p_1, \delta q_2, \delta p_2)^\top$ with $\delta x = \frac{1}{\sqrt{2}}(\delta a + \delta a^\dagger)$, $\delta y = \frac{1}{\sqrt{2}i}(\delta a - \delta a^\dagger)$, Eq. (14) can be written as [61–64]

$$\dot{u} = Mu + n, \tag{15}$$

where $n = (\sqrt{2\kappa}x^{\text{in}}, \sqrt{2\kappa}y^{\text{in}}, 0, \xi_1, 0, \xi_2)^\top$ is the noise vector and $x^{\text{in}} = \frac{1}{\sqrt{2}}(a^{\text{in}} + a^{in\dagger})$, $y^{\text{in}} = \frac{1}{\sqrt{2}i}(a^{\text{in}} - a^{in\dagger})$. $M$ is a time-dependent matrix,

$$M = \begin{pmatrix} B_- & A_- & -\sqrt{2}g\alpha_I & 0 & -\sqrt{2}g\alpha_I & 0 \\ A_+ & B_+ & \sqrt{2}g\alpha_R & 0 & \sqrt{2}g\alpha_R & 0 \\ 0 & 0 & 0 & \omega_1 & 0 & 0 \\ \sqrt{2}g\alpha_R & \sqrt{2}g\alpha_I & -\omega_1 & -\gamma_1 & \mu & 0 \\ 0 & 0 & 0 & 0 & 0 & \omega_2 \\ \sqrt{2}g\alpha_R & \sqrt{2}g\alpha_I & \mu & 0 & -\omega_2 & -\gamma_2 \end{pmatrix}, \tag{16}$$

with $A_\pm = \pm\{\Delta[1+\eta_c\cos(\Omega_c t)] + g\bar{q}_j + 4\chi|\alpha|^2\} + 2\chi[\alpha_R^2 - \alpha_I^2]$, $B_\pm = -\kappa \pm 4\chi\alpha_R\alpha_I$, $\alpha_R = \text{Re}(\alpha)$ and $\alpha_I = \text{Im}(\alpha)$. The evolution of matrix $M(t)$ can be derived from solving Eq. (13).

Then, we define a $6\times 6$ covariance matrix which contains fluctuation operators,

$$V_{ij} \equiv \frac{1}{2}\langle u_i u_j + u_j u_i\rangle. \tag{17}$$

So, the definition of $S_q$ and $S_q^\phi$ can be rewritten as

$$S_q = \left[\tfrac{1}{2}(V_{33} + V_{44} + V_{55} + V_{66} - V_{35} - V_{53} - V_{46} - V_{64})\right]^{-1},$$
$$S_q^\phi = \left[\tfrac{1}{2}(V_{33} + V_{44} + V_{55} + V_{66} + 2V_{45}\sin\phi - 2V_{36}\sin\phi - 2V_{46}\cos\phi - 2V_{35}\cos\phi)\right]^{-1}. \quad (18)$$

By substituting Eqs. (15) and (17) into the covariance matrix, we can get the time evolution of $V$ [33,61–64],

$$\dot{V} = MV + VM^T + N. \quad (19)$$

Here, $N = \mathrm{diag}[\kappa, \kappa, 0, \gamma_1(2\bar{n}_{\mathrm{bath}} + 1), 0, \gamma_2(2\bar{n}_{\mathrm{bath}} + 1)]$ is the noise matrix, satisfying $N_{ij}\delta(t-t') = \frac{1}{2}\langle\hat{\xi}_i(t)\hat{\xi}_j(t') + \hat{\xi}_j(t')\hat{\xi}_i(t)\rangle$.

By Eqs. (19) and (18), the evolution of the two synchronization measures can be derived. In addition, we redefine the synchronization measure $S_q^{(\phi)}$ as the calculated time-averaged synchronization $\lim_{T\to\infty}\frac{1}{T}\int_0^T S_q^{(\phi)}(t)dt$ in the asymptotic steady state of the system.

### B. Perfect quantum $\phi$ synchronization and quantum synchronization

To underscore the importance of quantum $\phi$ synchronization, we first investigate the time evolution of quantum synchronization $S_q$ and quantum $\phi$ synchronization $S_q^\phi$ under different parameter configurations. The parameters considered as variables include two periodic modulation methods (periodic modulation on cavity detuning and driving amplitude), the nonlinear coefficient $\chi$, and the direct coupling intensity of the two mechanical oscillators, denoted as $\mu$.

Under specific parameter settings, both quantum $\phi$ synchronization and quantum synchronization can reach stable states without direct coupling of the two mechanical oscillators, as shown by the limit-cycle trajectory of two mechanical oscillators in the phase space of Fig. 2(a). The parameters selected in Fig. 2 are similar to those in Refs. [2,31,45,59,62,65,66]. After a procedure of the parameters optimization and selection in the reasonable range, the optimal values of quantum synchronization and quantum $\phi$ synchronization are $S_q = 0.94$ and $S_q^\phi = 0.87$ on the steady state, as shown in Figs. 2(b) and 2(c), which illustrate that both the quantum synchronization and quantum $\phi$ synchronization are nearly perfect. However, even though $\bar{q}_1(t)$ and $\bar{q}_2(t)$ exhibit steady oscillations, their evolutions are not identical, as shown in Fig. 2(d), as well as the evolutions of $\bar{p}_1(t)$ and $\bar{p}_2(t)$ in Fig. 2(e). Their mean values have a small phase difference, $\phi = -0.24\pi$. The condition stated in Eq. (3) is not satisfied. As a result, no matter how perfect quantum synchronization may be, it lacks significance. Consequently, in this scenario, it becomes imperative to employ quantum $\phi$ synchronization with a phase offset of $\phi = -0.24\pi$ to investigate the synchronization between the two mechanical oscillators.

Next, we demonstrate the equivalence between these two measures of synchronization in the context of mean-value synchronization by introducing a direct coupling between the two mechanical oscillators. As shown in Figs. 3(b) and 3(c), the value of $S_q$ is 0.93 and $S_q^\phi$ is enhanced from 0.87 to 0.94 when compared to that in Fig. 2(c), owing to the coupling between the two oscillators. The phase difference $\phi$ between the two mechanical oscillators is $\phi = 0.05\pi$. The oscillation of the mean value of the position $\bar{q}(t)$, as well as the mean values of the momentum $\bar{p}(t)$, are nearly synchronized, as shown in

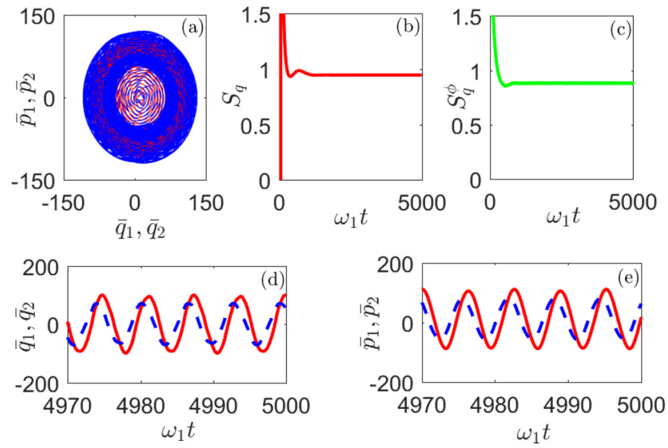

FIG. 2. (a) The evolution of the mean values $\bar{q}_1, \bar{q}_2$ and $\bar{p}_1, \bar{p}_2$ (dimensionless variables) of the two mechanical oscillators' position and momentum (blue and red lines). (b) Time evolution of $S_q(t)$. (c) Time evolution of $S_q^\phi(t)$. (d) Time evolution of the mean value $\bar{q}_1(t)$ (red solid line) and $\bar{q}_2(t)$ (blue dashed line). (e) Time evolution of the mean value $\bar{p}_1(t)$ (red solid line) and $\bar{p}_2(t)$ (blue dashed line). Here, we set $\omega_1 = 1$ as a reference unit of frequency, and the other parameters that have been used in the simulation are $\omega_2 = 1.0025\omega_1$, $\eta_c = 1.5\omega_1$, $\Omega_c = 3\omega_1$, $\eta_D = 0.65\omega_1$, $\Omega_D = 2.5\omega_1$, $\triangle = 1.5\omega_1$, $E = 210\omega_1$, $\chi = 0.00033\omega_1$, $\mu = 0$, $g = 0.003\omega_1$, $k = 0.15\omega_1$, and $\gamma_1 = \gamma_2 = 0.005\omega_1$. In all of the plots, time is in units of $\omega_1$.

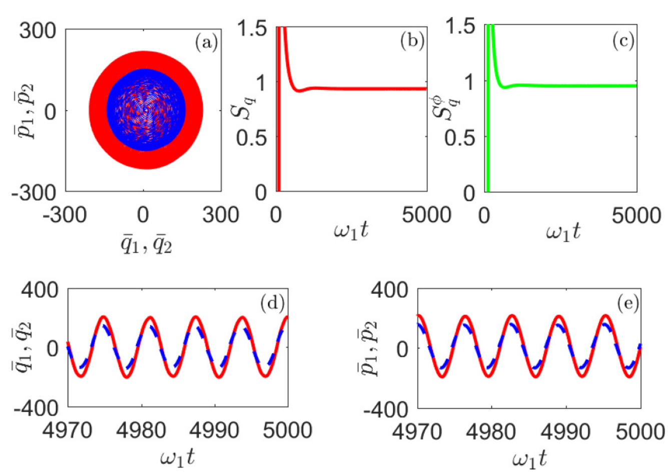

FIG. 3. (a) The evolution of the mean values $\bar{q}_1, \bar{q}_2$ and $\bar{p}_1, \bar{p}_2$ (dimensionless variables) of the two mechanical oscillators' position and momentum (blue and red lines). (b) Time evolution of $S_q(t)$. (c) Time evolution of $S_q^\phi(t)$. (d) Time evolution of the mean value $\bar{q}_1(t)$ (red solid line) and $\bar{q}_2(t)$ (blue dashed line). (e) Time evolution of the mean value $\bar{p}_1(t)$ (red solid line) and $\bar{p}_2(t)$ (blue dashed line). Here, we set $\omega_1 = 1$ as a reference unit of frequency, and the other parameters that have been used in the simulation are $\omega_2 = 1.0025\omega_1$, $\eta_c = 1.5\omega_1$, $\Omega_c = 3\omega_1$, $\eta_D = 0.65\omega_1$, $\Omega_D = 2.5\omega_1$, $\triangle = 1.5\omega_1$, $E = 210\omega_1$, $\chi = 0.00033\omega_1$, and $\mu = 0.01\omega_1$. In all of the plots, time is in units of $\omega_1$. Other parameters are the same as in Fig. 2.

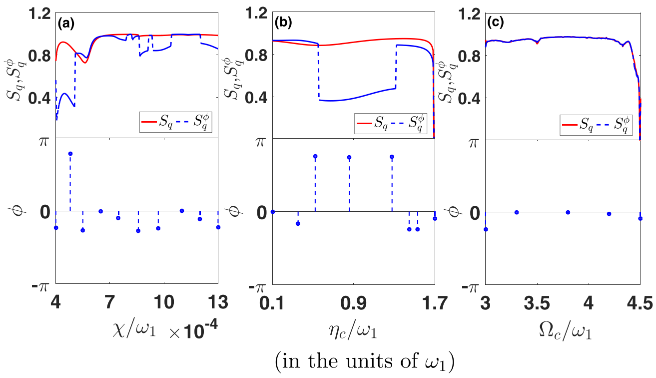

FIG. 4. The quantum synchronization measure $S_q$ (red solid line), quantum $\phi$ synchronization measure $S_q^\phi$ (blue dashed line), and discontinuity points of phase $\phi$ as a function of (a) Kerr nonlinear coefficient $\chi$ with $\eta_c = 1.5\omega_1$, $\Omega_c = 3\omega_1$, $\eta_D = 0.65\omega_1$, $\Omega_D = 2.5\omega_1$, (b) the amplitude $\eta_c$ of the cavity detuning modulation with $\Omega_c = 3\omega_1$, and (c) the frequency $\Omega_c$ of the cavity detuning with $\eta_c = 1.5\omega_1$. The other parameters are the same as in Fig. 2.

Figs. 3(d) and 3(e). In this scenario, both the conditions for quantum synchronization and quantum $\phi$ synchronization are met, rendering both synchronization metrics valid. Evidently, the coupling between the two mechanical oscillators assumes a pivotal role in achieving mean-value synchronization and elevating quantum $\phi$ synchronization in the nonlinear system.

In the aforementioned two scenarios, it becomes evident that quantum $\phi$ synchronization holds greater validity when the two mechanical oscillators have a phase difference $\phi$. Furthermore, it exhibits similarity to quantum synchronization in cases where mean-value synchronization is satisfied for $\phi = 0$.

### C. The response of two synchronization measures to different parameter configurations

To further investigate the universality of quantum $\phi$ synchronization compared to quantum synchronization in terms of the mean-value incomplete synchronization with a change of parameters, we next study how these two synchronization measures and the phase difference $\phi$ respond to changes in the system parameters. As shown in the top panel of Fig. 4(a), both quantum synchronization and quantum $\phi$ synchronization can be enhanced by increasing the nonlinear intensity $\chi$. Compared to the quantum synchronization measure $S_q$, the quantum $\phi$ synchronization measure $S_q^\phi$ exhibits some discontinuities with changes in nonlinear intensity. These turning points are attributed to the existence of phase difference $\phi$ between the two oscillators, as shown in the bottom panel of Fig. 4(a). As we discussed, in the case of nonzero $\phi$, even if the quantum synchronization measure is more stable, it is still invalid since the mean value is not synchronized. The quantum $\phi$ synchronization is more applied to arbitrary $\phi$. With the change of the Kerr nonlinear intensity $\chi$, different $\phi$ is generated and the behaviors of $\phi$ are correlated to nonlinear intensity $\chi$ with great sensitivity. In addition, these two quantum synchronizations can both reach the perfect synchronization for several nonlinear intensities $\chi$ as $\phi = 0$. When $\chi = 0.0007\omega_1$, the values of both the quantum synchronization measure and quantum $\phi$ synchronization measure reach 0.9, i.e., perfect quantum synchronization.

To sum up, both of the degrees of two synchronization measures can be enhanced in the nonlinear system for appropriate parameters [32,33]. However, the impressionable phase difference $\phi$ between the two mechanical oscillators results in a sensitivity enhancement of quantum $\phi$ synchronization compared with quantum synchronization. Next, we study the effects of the two different types of periodical modulations, i.e., cavity detuning and driving laser, on two synchronization measures. As shown in the top panel of Fig. 4(b), the similar discontinuous phenomenon of $S_q^\phi$ as in Fig. 4(a) can be observed with the changes of cavity modulation amplitudes $\eta_c$. The quantum $\phi$ synchronization deviates from quantum synchronization $S_q$, when $\eta_c$ is in the range of $0.5\omega_1$ to $1.3\omega_1$, and the value of $S_q^\phi$ has a sudden jump, corresponding to the flips of the phase difference $\phi$ in the same range of amplitude of modulation on cavity $\eta_c$ as shown in the bottom panel of Fig. 4(b). Therefore, within the range of $0.5\omega_1$ to $1.3\omega_1$, the sensitivity of the variable $S_q^\phi$ to the phase difference $\phi$ is increased under the influence of the cavity modulation amplitude $\eta_c$. It is easy to observe that the phenomenon of a phase flip occurs when the phase difference $\phi$ between the two mechanical oscillators transitions approximately from 0 to $\pi$. This is a classical nonlinear behavior induced by the amplitudes of periodic modulation within the cavity. Consequently, we can predict synchronization behaviors by examining the phase difference $\phi$ between the two oscillators.

While the above analysis indicates that quantum $\phi$ synchronization is notably influenced by the nonlinear strength $\chi$ and the cavity modulation amplitude $\eta_c$ in a nonlinear optomechanical system, it remains highly stable about the cavity modulation frequency $\Omega_c$. As shown in Fig. 4(c), the time evolution of two synchronization measures nearly coincides for $\Omega_c$, and it reveals the expected agreement of two synchronization measures under the influence of modulation frequency on the cavity, which indicates that the mean values of two mechanical oscillators are completely synchronized with phase difference $\phi = 0$. As we introduced in Sec. II, when $\phi = 0$, quantum synchronization is equal to quantum $\phi$ synchronization. When $\Omega_c/\omega_1 < 4.3$, two measures and $\phi$ are not sensitive to modulation frequency $\Omega_c$. The values of the two synchronization measures remain unchanged and accordant with each other, resulting from the phase difference being independent $\phi = 0$ without any variation. As $\Omega_c/\omega_1$ exceeds 4.3, both $S_q$ and $S_q^\phi$ exhibit a significant decrease, leading to a deterioration in quantum synchronization. This means that proper parameters with $\eta_c = 1.5\omega_1$, $\Omega_c = 3\omega_1$ are an essential precondition for perfect synchronization.

Similar to the cavity modulation, the periodical modulation of the driving laser can also affect the quantum synchronization $S_q$ and quantum $\phi$ synchronization $S_q^\phi$. As shown in Fig. 5(a), the value of quantum synchronization is better when $\eta_D/\omega_1$ is in a small range of 0.1 to 0.7. As the amplitude of the driving laser modulation $\eta_D$ increases, the quantum synchronization measure $S_q$ is nearly unchanged. The quantum $\phi$ synchronization initially coincides with quantum synchronization at $\phi = 0$. Subsequently, when $\eta_D/\omega_1$ is in the range of 0.3 to 0.4, it diminishes due to the presence of a phase difference $\phi$ between the two oscillators. This

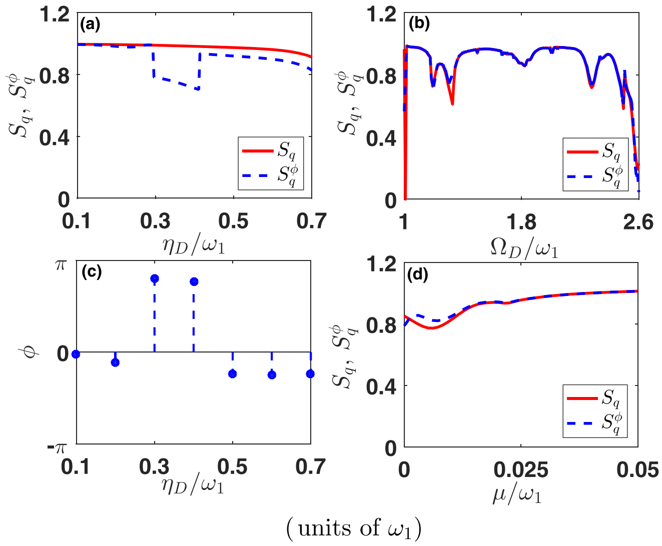


FIG. 5. The quantum synchronization measure $S_q$ (red solid line), quantum $\phi$ synchronization measure $S_q^\phi$ (blue dashed line), and discontinuity points of phase $\phi$ as a function of (a) the amplitude of the driving laser modulation $\eta_D$ with $\Omega_D = 2.5\omega_1$, (b) the frequency $\Omega_D$ of the driving laser modulation with $\eta_D = 0.65\omega_1$, (c) discontinuity points of phase $\phi$ as a function of the amplitude $\eta_D$ of the driving laser modulation with $\Omega_D = 2.5\omega_1$, and (d) direct coupling $\mu$ between the two mechanical oscillators with $\omega_2 = 1.005\omega_1$. The other parameters are the same as in Fig. 2.

phenomenon is also evident in Fig. 5(c), where the noticeable jump in $S_q^\phi$ corresponds to the transition of $\phi$ from $-0.11\pi$ to $0.8\pi$. Similarly, when $\eta_D = 0.4\omega_1$, the straight rise of the $S_q^\phi$ corresponds to the flip of phase difference $\phi$, transiting from $0.77\pi$ to $-0.25\pi$. It indicates that $\phi$ becomes sensible under the influence of $\eta_D$ for the same parameters regime. After $\eta_D/\omega_1 > 0.4$, the two lines are almost parallel to each other, which indicates that the phase difference is a fixed value with $\phi = -0.25\pi$ and is not affected by the amplitude of driving laser $\eta_D$. In general, similar to the case in modulation on cavity detunings, the sudden variation of $S_q^\phi$ is involved in the transition of phase difference $\phi$.

Furthermore, as shown in Fig. 5(b), both $S_q$ and $S_q^\phi$ exhibit significant fluctuations in response to the modulation frequency $\Omega_D$. The system is sensitive under the modulation of driving laser $\Omega_D$. Although the two synchronization measures can reach the same sensitivity, the phase difference $\phi$ is not susceptible to the parameter $\Omega_D$, which $\phi$ is always equal to 0 and remains unchanged as the two lines for the two quantum synchronization measures coincide with each other. Therefore, we can choose $\eta_D = 0.65\omega_1$, $\Omega_D = 2.5\omega_1$ as the optimal parameters for better quantum synchronization. And, we consider the direct coupling term $\mu q_1 q_2$ through a phonon tunneling. As shown in Fig. 5(d), it is shown that the value of $S_q$ and $S_q^\phi$ can be slightly enhanced, with increasing the coupling parameters $\mu$, and a better quantum synchronization can be reached.

Moreover, as shown in Fig. 6, we have performed the two synchronization measures $S_q$ and $S_q^\phi$ versus optomechanical coupling $g$ in Fig. 6(a) and optical detunings $\Delta$ in Fig. 6(b) for the optimal modulation parameter configurations. Figure 6(a)

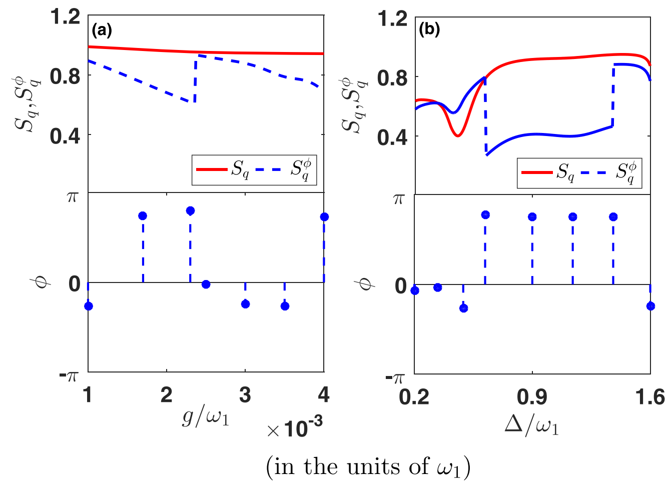


FIG. 6. The quantum synchronization measure $S_q$ (red solid line), quantum $\phi$ synchronization measure $S_q^\phi$ (blue dashed line), and discontinuity points of phase $\phi$ as a function of (a) the optomechanical coupling $g$ and (b) the optical detunings $\Delta$ under the optimal modulation parameter configurations. The other parameters are the same as in Fig. 2.

reveals that the quantum synchronization $S_q$ remains stable at 0.9 against the optomechanical coupling $g$. However, the quantum $\phi$ synchronization $S_q^\phi$ behaves differently, i.e., the value of $S_q^\phi$ decays with increasing coupling strength $g$. Notice that it exhibits a direct rise at $g = 2.3 \times 10^{-3}\omega_1$ and the step is followed by a continuous decline. The discontinuity of $S_q^\phi$ corresponds to the existence of phase $\phi$, as depicted in the bottom panel of Fig. 6(a). The effects of optical detunings $\Delta$ are displayed in Fig. 6(b); within the range of $0.65\omega_1$ to $1.4\omega_1$, quantum $\phi$ synchronization $S_q^\phi$ is separated from quantum synchronization $S_q$. At the boundary of this range ($0.65\omega_1 \sim 1.4\omega_1$), the great leap resulting from the phase $\phi$ between the two mechanical oscillators, as depicted in the bottom panel of Fig. 6(b), implies that the results of $S_q^\phi$ are more susceptible to optical detunings $\Delta$ compared with $S_q$. When the phase $\phi$ disappears, it indicates that mean-value synchronization is achieved, resulting in a consistency between the two synchronization measures.

After the parameters selection in the reasonable range, we have found a set of optimized parameters, i.e., $\eta_c = 1.5\omega_1$, $\Omega_c = 3\omega_1$, $\eta_D = 0.65\omega_1$, $\Omega_D = 2.5\omega_1$, $\chi = 0.00033\omega_1$, $\Delta = 1.5\omega_1$, $g = 0.003\omega_1$, and $E = 210\omega_1$, in which perfect quantum synchronization and quantum $\phi$ synchronization can be achieved. Therefore, quantum synchronization or quantum $\phi$ synchronization can be enhanced with optimal parameters, which is better than in the linear system with the same parameters [32,33].

### D. The experimental realization of the investigated optomechanical system

Based on our previous considerations, we briefly discuss the experimental parameter setting and the experimental realization in the investigated optomechanical system. In our simulations, we have adopted the dimensionless parameters that are similar to Mari's work [2], and these parameters can also be applied in the relevant experiments of most optomechanical systems. We have chosen reasonable experimental parameters from current experiments [62,66,67]. The optomechanical system consists of two mechanical oscillators and a Fabry-Pérot cavity of length $L$ and finesse $F$. We assume that $L = 25$ mm, $F = 2 \times 10^4$, $\omega_1 = 2\pi$ MHz, $\omega_2 = 2\pi \times 1.003$ MHz, $m = 40 \sim 150$ ng, $\gamma_j = 5 \times 10^{-3}\omega_1$, and $g = 3 \times 10^{-3}\omega_1$. The decay rate of the cavity mode is defined as $\kappa = \pi c/(2FL)$ ($c$ is the speed of light). The coupling interaction between the two mechanical oscillators through a phonon tunneling is also studied in some research [2,68]. The mechanical modes are placed in the middle of the optical cavity, and the cavity mode is driven by a red-detuned laser $\Delta \simeq \omega_1$ with the wavelength $\lambda = 1064$ nm. The intensity of the driving field is $E_0$, while it has a periodical modulation of frequency $\Omega_D$ and amplitude $\eta_D$, $E = E_0[1 + \eta_D \cos(\Omega_D t)] = E_0 + E_1 \cos(\Omega_D t)$, and the modulation coefficients $E_n$ are given by $E_n = \sqrt{2\kappa P_n/(\hbar\omega_L)}$ which corresponds to the power with $P_0 = 10$ mw and the modulation sidebands equal to $P_1 = 2$ mW [3,62]. The periodical modulation of cavity detuning can be realized by the piezoelectric transducer, which can apply to the periodic modifications of cavity lengths through converting the electrical signal to mechanical vibration [69].

Then, we briefly present an experimental realization in the investigated optomechanical system. Various experimental research has facilitated the coupling of optomechanical systems via the interaction between cavities or mechanical oscillators [4,70]. Likewise, the implementation of micromechanical oscillator arrays has also been achieved in recent studies [71]. Meanwhile, quantum correlations have already been studied in experiments, and some studies have proposed an experimental scheme to characterize the entangled state [72] and measure the chaos of the cavity [73]. Our studies focus on a theoretical model constituted of a driven high-finesse Fabry-Pérot cavity containing two coupled mechanical oscillators, and the corresponding experiments have been successfully carried out [74–76]. To investigate the properties of the optical and mechanical in an optomechanical system, we have introduced a similar method to that proposed in Refs. [75,76]. We utilize a laser beam with the wavelength of $\lambda = 1064$ nm. The laser beam splits into two beams: one is a probe beam modulated by an electro-optical modulator (EOM), and the other is a pump beam modulated by an acousto-optic modulator (AOM) with detuning $\Delta$ from the cavity to facilitate optomechanical interaction and achieve the mechanical modes driven by laser beams. The reflected probe beam has two effects: one is used to lock the cavity to the laser frequency by using the Pound-Drever-Hall technique, and the other is used to analyze the motions of mechanical oscillators through homodyne detection.

In our scheme, we also study the effects of second-order nonlinearity $\chi$ on quantum synchronization and quantum $\phi$ synchronization. The cavity is filled with a Kerr-type medium, and the nonlinearity of the optomechanical interaction of the quantum level is taken into account. Moreover, the second-order nonlinearity $\chi$ has been theoretically and experimentally introduced to different schemes in an optomechanical system, including photon blockade [77,78] and chaos [79]. We have adopted the experimental parameter from the study [80] and the second-order nonlinearity is $\chi \sim 0.4\pi$ kHz and $\chi/\omega_1 \sim 10^{-4}$, which is close to the parameters in our numerical simulation.

## IV. CONCLUSIONS

In summary, we have proposed an optomechanical system composed of one cavity and two oscillators to study the response of quantum synchronization and quantum $\phi$ synchronization to different parameters. The values of quantum synchronization and quantum $\phi$ synchronization are different under some specific parameters; the underlying physical mechanism is the appearance of phase difference $\phi$ between the two mechanical oscillators. Then the sensitivity of two synchronization measures to different parameters is compared and discussed. We have found that the phase difference $\phi$ is susceptible to Kerr nonlinear coefficient $\chi$, amplitude $\eta_c$ and $\eta_D$ of two periodical modulation ways, detuning $\Delta$, and optomechanical coupling $g$, resulting in a sharp drop or straight rise of quantum $\phi$ synchronization.

However, under the influence of modulation frequency $\Omega_c$ and direct coupling $\mu$ on the cavity, the values of quantum synchronization and quantum $\phi$ synchronization are the same, resulting from the phase difference $\phi$ stably tending to 0, and it shows that phase difference $\phi$ in this optomechanical system remains practically unaffected by the modulation frequency. Although the system is sensitive to modulation frequency $\Omega_D$ on the driving field and the values of quantum synchronization and quantum $\phi$ synchronization have some fluctuations, the $\phi$ is not susceptible and steadily approaches 0. Finally, we can find the optimal parameters to achieve good quantum synchronization and quantum $\phi$ synchronization. Therefore, it is worth studying quantum synchronization and other quantum effects in a Kerr nonlinear medium, as it has some profound impacts on quantum correlations.

## ACKNOWLEDGMENT

This work is supported by the National Natural Science Foundation of China (NSFC) (Grants No. 11875103 and No. 12147206).

[1] C. Huygens, *uvres Complètes de Christiaan Huygens* (Martinus Nijhoff, The Hague, 1893), Vol. 15.

[2] A. Mari, A. Farace, N. Didier, V. Giovannetti, and R. Fazio, Measures of quantum synchronization in continuous variable systems, Phys. Rev. Lett. **111**, 103605 (2013).

[3] L. Ying, Y.-C. Lai, and C. Grebogi, Quantum manifestation of a synchronization transition in optomechanical systems, Phys. Rev. A **90**, 053810 (2014).

[4] M. Aspelmeyer, T. J. Kippenberg, and F. Marquardt, Cavity optomechanics, Rev. Mod. Phys. **86**, 1391 (2014).

[5] O. V. Zhirov and D. L. Shepelyansky, Quantum synchronization and entanglement of two qubits coupled to a driven dissipative resonator, Phys. Rev. B **80**, 014519 (2009).

[6] V. Ameri, M. Eghbali-Arani, A. Mari, A. Farace, F. Kheirandish, V. Giovannetti, and R. Fazio, Mutual information as an order parameter for quantum synchronization, Phys. Rev. A **91**, 012301 (2015).

[7] M. Xu, D. A. Tieri, E. C. Fine, J. K. Thompson, and M. J. Holland, Synchronization of two ensembles of atoms, Phys. Rev. Lett. **113**, 154101 (2014).

[8] M. Xu and M. J. Holland, Conditional Ramsey spectroscopy with synchronized atoms, Phys. Rev. Lett. **114**, 103601 (2015).

[9] M. R. Hush, W. Li, S. Genway, I. Lesanovsky, and A. D. Armour, Spin correlations as a probe of quantum synchronization in trapped-ion phonon lasers, Phys. Rev. A **91**, 061401(R) (2015).

[10] T. E. Lee, C.-K. Chan, and S. Wang, Entanglement tongue and quantum synchronization of disordered oscillators, Phys. Rev. E **89**, 022913 (2014).

[11] S. Walter, A. Nunnenkamp, and C. Bruder, Quantum synchronization of a driven self-sustained oscillator, Phys. Rev. Lett. **112**, 094102 (2014).

[12] T. E. Lee and H. R. Sadeghpour, Quantum synchronization of quantum van der Pol oscillators with trapped ions, Phys. Rev. Lett. **111**, 234101 (2013).

[13] M. Samoylova, N. Piovella, G. R. M. Robb, R. Bachelard, and P. W. Courteille, Synchronization of Bloch oscillations by a ring cavity, Opt. Express **23**, 14823 (2015).

[14] Y. Gül, Synchronization of networked Jahn-Teller systems in squids, Intl. J. Mod. Phys. B **30**, 1650125 (2016).

[15] F. Quijandría, D. Porras, J. J. García-Ripoll, and D. Zueco, Circuit QED bright source for chiral entangled light based on dissipation, Phys. Rev. Lett. **111**, 073602 (2013).

[16] W. Li, C. Li, and H. Song, Quantum synchronization and quantum state sharing in an irregular complex network, Phys. Rev. E **95**, 022204 (2017).

[17] G. Manzano, F. Galve, G. L. Giorgi, E. Hernández-Garcá, and R. Zambrini, Synchronization quantum correlations and entanglement in oscillator networks, Sci. Rep. **3**, 1439 (2013).

[18] J. Nokkala, F. Galve, R. Zambrini, S. Maniscalco, and J. Piilo, Complex quantum networks as structured environments: engineering and probing, Sci. Rep. **6**, 26861 (2016).

[19] S. Dutta and N. R. Cooper, Critical response of a quantum van der Pol oscillator, Phys. Rev. Lett. **123**, 250401 (2019).

[20] M. H. Matheny, M. Grau, L. G. Villanueva, R. B. Karabalin, M. C. Cross, and M. L. Roukes, Phase synchronization of two anharmonic nanomechanical oscillators, Phys. Rev. Lett. **112**, 014101 (2014).

[21] L. M. Pecora and T. L. Carroll, Synchronization in chaotic systems, Phys. Rev. Lett. **64**, 821 (1990).

[22] J. Zhang, Y.-X. Liu, Ş. K. Özdemir, R.-B. Wu, F. Gao, X.-B. Wang, L. Yang, and F. Nori, Quantum internet using code division multiple access, Sci. Rep. **3**, 2211 (2013).

[23] C.-L. Zhu, N. Yang, Y.-X. Liu, F. Nori, and J. Zhang, Entanglement distribution over quantum code-division multiple-access networks, Phys. Rev. A **92**, 042327 (2015).

[24] F. Bemani, A. Motazedifard, R. Roknizadeh, M. H. Naderi, and D. Vitali, Synchronization dynamics of two nanomechanical membranes within a Fabry-Perot cavity, Phys. Rev. A **96**, 023805 (2017).

[25] C.-S. Hu, L.-T. Shen, Z.-B. Yang, H. Wu, Y. Li, and S.-B. Zheng, Manifestation of classical nonlinear dynamics in optomechanical entanglement with a parametric amplifier, Phys. Rev. A **100**, 043824 (2019).

[26] A. Roulet and C. Bruder, Quantum synchronization and entanglement generation, Phys. Rev. Lett. **121**, 063601 (2018).

[27] D. Stefanatos, Maximising optomechanical entanglement with optimal control, Quantum Sci. Technol. **2**, 014003 (2017).

[28] G. L. Giorgi, F. Galve, G. Manzano, P. Colet, and R. Zambrini, Quantum correlations and mutual synchronization, Phys. Rev. A **85**, 052101 (2012).

[29] G. L. Giorgi, F. Plastina, G. Francica, and R. Zambrini, Spontaneous synchronization and quantum correlation dynamics of open spin systems, Phys. Rev. A **88**, 042115 (2013).

[30] C.-G. Liao, R.-X. Chen, H. Xie, M.-Y. He, and X.-M. Lin, Quantum synchronization and correlations of two mechanical resonators in a dissipative optomechanical system, Phys. Rev. A **99**, 033818 (2019).

[31] G. J. Qiao, H. X. Gao, H. D. Liu, and X. X. Yi, Quantum synchronization of two mechanical oscillators in coupled optomechanical systems with kerr nonlinearity, Sci. Rep. **8**, 15614 (2018).

[32] H. Geng, L. Du, H. D. Liu, and X. X. Yi, Enhancement of quantum synchronization in optomechanical system by modulating the couplings, J. Phys. Commun. **2**, 025032 (2018).

[33] L. Du, C.-H. Fan, H.-X. Zhang, and J.-H. Wu, Synchronization enhancement of indirectly coupled oscillators via periodic modulation in an optomechanical system, Sci. Rep. **7**, 15834 (2017).

[34] P. Djorwé, Y. Pennec, and B. Djafari-Rouhani, Self-organized synchronization of mechanically coupled resonators based on optomechanics gain-loss balance, Phys. Rev. B **102**, 155410 (2020).

[35] P. Djorwe, Y. Pennec, and B. Djafari-Rouhani, Frequency locking and controllable chaos through exceptional points in optomechanics, Phys. Rev. E **98**, 032201 (2018).

[36] M.-C. Ho, Y.-C. Hung, and C.-H. Chou, Phase and anti-phase synchronization of two chaotic systems by using active control, Phys. Lett. A **296**, 43 (2002).

[37] M. G. Rosenblum, A. S. Pikovsky, and J. Kurths, Phase synchronization of chaotic oscillators, Phys. Rev. Lett. **76**, 1804 (1996).

[38] G. V. Osipov, A. S. Pikovsky, and J. Kurths, Phase synchronization of chaotic rotators, Phys. Rev. Lett. **88**, 054102 (2002).

[39] U. Parlitz, L. Junge, W. Lauterborn, and L. Kocarev, Experimental observation of phase synchronization, Phys. Rev. E **54**, 2115 (1996).

[40] K. Wiesenfeld, P. Colet, and S. H. Strogatz, Frequency locking in Josephson arrays: Connection with the Kuramoto model, Phys. Rev. E **57**, 1563 (1998).

[41] J. Thévenin, M. Romanelli, M. Vallet, M. Brunel, and T. Erneux, Resonance assisted synchronization of coupled oscillators: Frequency locking without phase locking, Phys. Rev. Lett. **107**, 104101 (2011).

[42] W. Li, Analyzing quantum synchronization through Bohmian trajectories, Phys. Rev. A **106**, 023512 (2022).

[43] G. J. Qiao, X. Y. Liu, H. D. Liu, C. F. Sun, and X. X. Yi, Quantum $\phi$-synchronization in a coupled optomechanical system with periodic modulation, Phys. Rev. A **101**, 053813 (2020).

[44] C. Joshi, J. Larson, M. Jonson, E. Andersson, and P. Öhberg, Entanglement of distant optomechanical systems, Phys. Rev. A **85**, 033805 (2012).

[45] W. Li, P. Piergentili, J. Li, S. Zippilli, R. Natali, N. Malossi, G. Di Giuseppe, and D. Vitali, Noise robustness of synchronization of two nanomechanical resonators coupled to the same cavity field, Phys. Rev. A **101**, 013802 (2020).

[46] F. Marquardt, J. G. E. Harris, and S. M. Girvin, Dynamical multistability induced by radiation pressure in high-finesse micromechanical optical cavities, Phys. Rev. Lett. **96**, 103901 (2006).

[47] C. K. Law, Interaction between a moving mirror and radiation pressure: A Hamiltonian formulation, Phys. Rev. A **51**, 2537 (1995).

[48] D.-Y. Wang, C.-H. Bai, H.-F. Wang, A.-D. Zhu, and S. Zhang, Steady-state mechanical squeezing in a double-cavity optomechanical system, Sci. Rep. **6**, 38559 (2016).

[49] L. Jin, Y. Guo, X. Ji, and L. Li, Reconfigurable chaos in electro-optomechanical system with negative duffing resonators, Sci. Rep. **7**, 4822 (2017).

[50] D.-G. Lai, J.-F. Huang, X.-L. Yin, B.-P. Hou, W. Li, D. Vitali, F. Nori, and J.-Q. Liao, Nonreciprocal ground-state cooling of multiple mechanical resonators, Phys. Rev. A **102**, 011502(R) (2020).

[51] J. P. Mathew, J. Pino, and E. Verhagen, Synthetic gauge fields for phonon transport in a nano-optomechanical system, Nat. Nanotechnol. **15**, 198 (2020).

[52] A. Farace and V. Giovannetti, Enhancing quantum effects via periodic modulations in optomechanical systems, Phys. Rev. A **86**, 013820 (2012).

[53] C.-H. Bai, D.-Y. Wang, H.-F. Wang, A.-D. Zhu, and S. Zhang, Classical to quantum transition behavior between two oscillators separated in space under the action of optomechanical interaction, Sci. Rep. **7**, 2545 (2017).

[54] H. Jing, S. K. Özdemir, X.-Y. Lü, J. Zhang, L. Yang, and F. Nori, $\mathcal{PT}$-symmetric phonon laser, Phys. Rev. Lett. **113**, 053604 (2014).

[55] D. W. Schönleber, A. Eisfeld, and R. El-Ganainy, Optomechanical interactions in non-Hermitian photonic molecules, New J. Phys. **18**, 045014 (2016).

[56] V. Giovannetti and D. Vitali, Phase-noise measurement in a cavity with a movable mirror undergoing quantum Brownian motion, Phys. Rev. A **63**, 023812 (2001).

[57] Y.-C. Liu, Y.-F. Shen, Q. Gong, and Y.-F. Xiao, Optimal limits of cavity optomechanical cooling in the strong-coupling regime, Phys. Rev. A **89**, 053821 (2014).

[58] X.-W. Xu and Y. Li, Optical nonreciprocity and optomechanical circulator in three-mode optomechanical systems, Phys. Rev. A **91**, 053854 (2015).

[59] W. Li, C. Li, and H. Song, Quantum synchronization in an optomechanical system based on Lyapunov control, Phys. Rev. E **93**, 062221 (2016).

[60] A. Mari and J. Eisert, Opto-and electro-mechanical entanglement improved by modulation, New J. Phys. **14**, 075014 (2012).

[61] W. Li, C. Li, and H. Song, Criterion of quantum synchronization and controllable quantum synchronization based on an optomechanical system, J. Phys. B **48**, 035503 (2015).

[62] A. Mari and J. Eisert, Gently modulating optomechanical systems, Phys. Rev. Lett. **103**, 213603 (2009).

[63] G. Wang, L. Huang, Y.-C. Lai, and C. Grebogi, Nonlinear dynamics and quantum entanglement in optomechanical systems, Phys. Rev. Lett. **112**, 110406 (2014).

[64] J. Larson and M. Horsdal, Photonic Josephson effect, phase transitions, and chaos in optomechanical systems, Phys. Rev. A **84**, 021804(R) (2011).

[65] W. Li, W. Zhang, C. Li, and H. Song, Properties and relative measure for quantifying quantum synchronization, Phys. Rev. E **96**, 012211 (2017).

[66] M. Eichenfield, R. Camacho, J. Chan, K. J. Vahala, and O. Painter, A picogram- and nanometer-scale photonic-crystal optomechanical cavity, Nature (London) **459**, 550 (2009).

[67] M. Eichenfield, J. Chan, R. M. Camacho, K. J. Vahala, and O. Painter, Optomechanical crystals, Nature (London) **462**, 78 (2009).

[68] G. Heinrich, M. Ludwig, J. Qian, B. Kubala, and F. Marquardt, Collective dynamics in optomechanical arrays, Phys. Rev. Lett. **107**, 043603 (2011).

[69] J.-Q. Liao, C. K. Law, L.-M. Kuang, and F. Nori, Enhancement of mechanical effects of single photons in modulated two-mode optomechanics, Phys. Rev. A **92**, 013822 (2015).

[70] H. Okamoto, A. Gourgout, and C. Y. Chang, Coherent phonon manipulation in coupled mechanical resonators, Nat. Phys. **9**, 480 (2013).

[71] M. Zhang, S. Shah, J. Cardenas, and M. Lipson, Synchronization and phase noise reduction in micromechanical oscillator arrays coupled through light, Phys. Rev. Lett. **115**, 163902 (2015).

[72] D. Vitali, S. Gigan, A. Ferreira, H. R. Böhm, P. Tombesi, A. Guerreiro, V. Vedral, A. Zeilinger, and M. Aspelmeyer, Optomechanical entanglement between a movable mirror and a cavity field, Phys. Rev. Lett. **98**, 030405 (2007).

[73] Y.-H. Ma, R. Zhao, X.-W. Hou, J.-W. Liu, M.-X. Li, and X. Zhao, Chaos generation in opto-mechanical coupling system assisted by two-level atoms, Ann. Phys. **535**, 2200470 (2023).

[74] P. Piergentili, L. Catalini, M. Bawaj, S. Zippilli, N. Malossi, R. Natali, D. Vitali, and G. D. Giuseppe, Two-membrane cavity optomechanics, New J. Phys. **20**, 083024 (2018).

[75] X. Wei, J. Sheng, C. Yang, Y. Wu, and H. Wu, Controllable two-membrane-in-the-middle cavity optomechanical system, Phys. Rev. A **99**, 023851 (2019).

[76] P. Piergentili, W. Li, R. Natali, N. Malossi, D. Vitali, and G. D. Giuseppe, Two-membrane cavity optomechanics: Nonlinear dynamics, New J. Phys. **23**, 073013 (2021).

[77] Y. H. Zhou, H. Z. Shen, and X. X. Yi, Unconventional photon blockade with second-order nonlinearity, Phys. Rev. A **92**, 023838 (2015).

[78] D. Gerace and V. Savona, Unconventional photon blockade in doubly resonant microcavities with second-order nonlinearity, Phys. Rev. A **89**, 031803(R) (2014).

[79] H. Goto and T. Kanao, Chaos in coupled Kerr-nonlinear parametric oscillators, Phys. Rev. Res. **3**, 043196 (2021).

[80] X.-Y. Lü, J.-Q. Liao, L. Tian, and F. Nori, Steady-state mechanical squeezing in an optomechanical system via Duffing nonlinearity, Phys. Rev. A **91**, 013834 (2015).